Guided Ion Beam Studies of the Reactions of Ti^+, V^+, and Cr^+ with Silane. Electronic State Effects, Comparison to Reactions with Methane, and M^+-SiH_x ($x = 0-3$) Bond Energies

Bernice L. Kickel and P. B. Armentrout*

Contribution from the Department of Chemistry, University of Utah, Salt Lake City, Utah 84112

Received May 12, 1994®

Abstract: Guided ion beam techniques are used to measure cross sections as a function of kinetic energy for the reactions of $M^+ = Ti^+$, V^+, and Cr^+ with SiH_4. The major low-energy process in all three systems is formation of $MSiH_2^+ + H_2$. At higher energies, the formation of $MH^+ + SiH_3$ dominates the reactivity. Minor ionic products include $MSiH_x^+$ ($x = 0$, 1, 3), as well as SiH_3^+ in the V^+ and Cr^+ systems. Variation of source conditions allows the effect of electronic excitation on the reactivity of these systems to be studied. The results indicate that the reactions are more efficient for the low-spin doublet (Ti^+), triplet (V^+), and quartet (Cr^+) excited states. The reactivities of these systems may be understood in terms of simple molecular orbital concepts and spin conservation. The thresholds for the various reactions are evaluated to yield 0 K bond dissociation energies for M^+-Si, M^+-SiH, M^+-SiH_2, and M^+-SiH_3 of 2.54 ± 0.17, 2.30 ± 0.11, 2.17 ± 0.07, and 1.69 ± 0.18 eV, respectively, for M = Ti, of 2.37 ± 0.15, 2.09 ± 0.12, 2.02 ± 0.09, and 1.54 ± 0.16 eV, respectively, for M = V, and of 2.10 ± 0.16, 1.02 ± 0.29, 0.99 ± 0.14, and 0.78 ± 0.18 eV, respectively, for M = Cr. The present results are compared to those previously reported for the reactions of Ti^+, V^+, and Cr^+ with methane.

Introduction

Over the past thirty years, interest in transition-metal-silicon compounds in the condensed phase has grown steadily. Transition-metal-silicon complexes have been postulated as intermediates in a number of reactions such as hydrosilation,[1,2] silane polymerization,[3] and chemical vapor deposition of transition-metal silicides.[4] These processes can be quite complex, and fundamental information regarding such species would be useful in understanding their reactivity. Such information may be obtained from gas-phase studies, but these are not extensive at present. Kang *et al.* studied the reactions of transition-metal ions (Ti^+, V^+, Cr^+, Fe^+, Co^+, and Ni^+) with organosilanes in an ion beam apparatus.[5] They observed formation of transition-metal silylenes ($MSiH_2^+$) as major products, an observation with no precedent in condensed-phase chemistry. Geribaldi and coworkers made similar observations in the reactions of the group 3 metal ions with silane.[6] Bakhtiar *et al.*[7] have studied the generation and characterization of isomeric Fe^+-silene and -silylene complexes in the gas phase. Cundari and Gordon[8] have completed calculations regarding the bonding and electronic structure of the transition-metal-silicon double bond in $MSiH_2^+$. They concluded that $MSiH_2^+$ species have significantly weaker bonds (as estimated by force constants) than do their MCH_2^+ analogues.

In order to provide more comprehensive fundamental information on transition-metal-silicon species, we have initiated a series of studies to investigate the reactions of atomic transition-metal ions with silane. The present work includes Ti^+, V^+, and Cr^+, three metals previously found to have similar reactivities with small molecules,[9-12] and subsequent papers will extend these examinations to the group 3 and remaining first-row transition-metal ions.[13] The kinetic energy dependence of these reactions is analyzed to yield M^+-SiH_x ($x = 0-3$) bond energies and provide insight into the mechanisms for the reactions. By varying the ion source conditions, we can alter the amounts of excited electronic states present in the reactant ion beam, enabling us to determine the influence of different electronic states on the reactivity of the system. This can have a dramatic effect on metal ion reactivity as previously observed in reactions of these transition-metal ions with hydrogen, ammonia, and various hydrocarbon species.[10-12,14,15] It is also important to note that such gas-phase studies allow us to examine the intrinsic properties of metal-silicon chemistry without the complication of solution-phase phenomena. Comparison of transition-metal silicon vs transition-metal carbon bond energies provides insight into the effects of substitution of silicon for carbon.

Experimental Section

General. Complete descriptions of the apparatus and experimental procedures are given elsewhere.[16] Briefly, ions are produced as described below, accelerated, and focused into a magnetic sector

® Abstract published in *Advance ACS Abstracts,* October 15, 1994.

(1) Noll, W. *Chemistry and Technology of Silicons*; Academic: New York, 1986.

(2) Stone, F. G. A.; West, R., Eds. *Advances in Organometallic Chemistry*; Academic: San Diego, CA, 1990.

(3) For a review of polysilane polymers, see: West, R. *J. Organomet. Chem.* **1986**, *300*, 327.

(4) Corey, J. Y.; Corey, E. R.; Gaspar, P. P.; Eds. *Silicon Chemistry*; Harwood: Chichester, 1988; Chapters 30, 32, and 33.

(5) Kang, H.; Jacobson, D. B.; Shin, S. K.; Beauchamp, J. L.; Bowers, M. T. *J. Am. Chem. Soc.* **1986**, *108*, 5668.

(6) Decouzon, M.; Gal, J.-F.; Geribaldi, S.; Rouillard, M.; Sturla, J.-M. *Rapid Commun. Mass Spectrom.* **1989**, *3*, 298. Azzaro, M.; Breton, M.; Decouzon, M.; Geribaldi, S. *Rapid Commun. Mass Spectrom.* **1992**, *6*, 306.

(7) Bakhtiar, R.; Holznagel, C.; Jacobson, D. B. *J. Am. Chem. Soc.* **1993**, *115*, 345.

(8) Cundari, T. R.; Gordon, M. S. *J. Phys. Chem.* **1992**, *96*, 631.

(9) Elkind, J. L.; Armentrout, P. B. *J. Phys. Chem.* **1987**, *91*, 2037.

(10) Clemmer, D. E.; Sunderlin, L. S.; Armentrout, P. B. *J. Phys. Chem.* **1990**, *94*, 208.

(11) Clemmer, D. E.; Sunderlin, L. S.; Armentrout, P. B. *J. Phys. Chem.* **1990**, *94*, 3008.

(12) Armentrout, P. B. In *Selective Hydrocarbon Activation: Principles and Progress*; Davies, J. A., Watson, P. L., Greenberg, A., Liebman, J. F., Eds.; VCH: New York, 1990: pp 467-533.

(13) Kickel, B. L.; Armentrout, P. B. *J. Am. Chem. Soc.* Accepted for publication. Kickel, B. L.; Armentrout, P. B. Submitted for publication.

(14) Armentrout, P. B. *Science* **1991**, *251*, 175.

(15) Armentrout, P. B. *Annu. Rev. Phys. Chem.* **1990**, *41*, 313.

(16) Ervin, K. M.; Armentrout, P. B. *J. Chem. Phys.* **1985**, *83*, 166.

0002-7863/94/1516-10742$04.50/0

momentum analyzer for mass analysis. They are then decelerated to the desired translational energy and focused into an octopole ion beam guide[17] that traps ions in the radial direction. The octopole passes through a static gas cell into which the neutral gas is introduced at sufficiently low pressures, 0.05−0.15 mTorr, that multiple ion−molecule collisions are improbable. Pressure-dependent studies verify that the cross sections measured here are due to single ion−molecule interactions. After leaving the octopole, transmitted reactant and product ions are extracted and analyzed in a quadrupole mass filter. Ions are detected by a secondary electron scintillation ion counter by using pulse-counting techniques. Raw ion intensities are converted to absolute reaction cross sections as described previously with uncertainties estimated as ± 20%.[16]

Laboratory ion energies (lab) are converted to energies in the center-of-mass frame (CM) by using the conversion $E_{CM} = E_{lab}M/(m + M)$, where m is the mass of the ion and M is the mass of the neutral reactant. The absolute energy and energy distribution of the ions in the interaction region are measured by using the octopole as a retarding field analyzer.[16] These measurements show that the distribution of ion energies is Gaussian with a typical full-width at half-maximum (fwhm) of ~0.5 eV (lab). The uncertainty in the absolute energy scale is ±0.05 eV (lab). The thermal motion of the gas in the reaction cell has a distribution with a fwhm of $\sim 0.4E_{CM}^{1/2}$ eV.[18] At very low energies, the slower ions in the kinetic energy distribution of the beam are not transmitted through the octopole, resulting in a narrowing of the ion energy distribution. We take advantage of this effect to access very low interaction energies as described previously.[16,19]

Ion Source. A dc-discharge flow tube (DC/FT) ion source, described in detail previously,[20] is used to form Ti^+ and V^+ ions. The dc discharge is used to ionize and accelerate argon ions into a vanadium or titanium metal cathode to sputter off Ti^+ or V^+. The resulting ions are swept downstream in a flow of helium and argon at a total pressure of 0.4−0.7 Torr and encounter $>10^5$ collisions with the bath gases. It is believed that most excited-state V^+ and Ti^+ ions are quenched to their ground state by these collisions; however, more complete quenching of excited electronic states is accomplished by addition of small amounts of methane (3−5 mTorr) to the flow.[21,22] The efficiency of this quenching has been verified in previous studies.[23,24] We assume that a Maxwell−Boltzmann distribution at the ambient flow tube temperature of 300 K accurately describes the populations of the electronic states of the ions, as listed in Table 1.

Formation of ground state Cr^+ ions is accomplished in a surface ionization (SI) source. CrO_2Cl_2 is passed over a resistively heated rhenium filament at 1900 ± 100 K, as measured by optical pyrometry. Dissociation of CrO_2Cl_2 and ionization of the resultant chromium atoms occurs on the filament. We assume a Maxwell−Boltzmann distribution at the filament temperature accurately describes the populations of the electronic states, as listed in Table 1. The validity of this assumption has been discussed previously,[21] and recent work by van Koppen *et al.* has verified this assumption in the case of Co^+.[25]

An electron impact (EI) source is also used to produce Ti^+, V^+, and Cr^+ from $TiCl_4$, $VOCl_3$, and CrO_2Cl_2, respectively. The ionization of these compounds by EI at an electron energy of 30 eV has been characterized previously.[21,22,26,27] The populations of the electronic states produced in this source are also listed in Table 1.

Thermochemical Analysis. The threshold regions of the experimental reaction cross sections are analyzed by using the empirical model of eq 1.

Table 1. Electronic States of Ti^+, V^+ and Cr^+

	state	config	electron energy,[a] eV	% population FT or SI[b]	% population EI (30 eV)[c]
Ti^+	a^4F	$3d^24s$	0.028	98.44	80(3)
	b^4F	$3d^3$	0.135	1.56	
	a^2F	$3d^24s$	0.593		9(3)
	a^2D	$3d^24s$	1.082		
	a^2G	$3d^3$	1.124		
	Σ states >1.0 eV		1.18		11(4)
V^+	a^5D	$3d^4$	0.026	100.00	40
	a^5F	$3d^34s$	0.36		18
	a^3F	$3d^34s$	1.10		7
	a^3P	$3d^4$	1.45		10
	a^3H	$3d^4$	1.57		
	b^3F	$3d^4$	1.68		
	others	$3d^34s$	≥1.69		25
Cr^+	a^6S	$3d^5$	0.0	99.97	86(5)
	a^6D	$3d^44s$	1.52	0.03	13(5)
	a^4D	$3d^44s$	2.46		1
	a^4G	$3d^5$	2.56		

[a] Energies are a statistical over J levels taken from: Sugar, J.; Corliss, C. *J. Phys. Chem. Ref. Data* **1985**, *14*, Suppl. 2. [b] Maxwell−Boltzmann distribution for 300 K (FT, Ti and V) and 1900 K (SI, Cr). [c] EI populations are estimated from the diagnostic reaction of Ti^+ and V^+ with methane, refs 21 and 22, respectively, and by ion chromatography, ref 27.

$$\sigma(E) = \sigma_o \sum g_i (E + E_{rot} + E_i - E_0)^n / E \qquad (1)$$

Here, E is the relative kinetic energy, E_0 is the reaction endothermicity for reaction of the lowest J state of the ion at 0 K, σ_o is an energy-independent scaling factor, and n is an adjustable parameter. This equation takes the internal energy of the SiH_4 reagent into consideration by including the average rotational energy, $E_{rot}(SiH_4) = 3kT/2 = 0.039$ eV at 300 K. Vibrational energy contributions are negligible (<0.007 eV). The summation is over the distribution of electronic states i of the metal ion reactant having energies E_i (Table 1 gives J-averaged values) and relative populations g_i, where $\Sigma g_i = 1$. The resulting model cross section is then convoluted with the ion and neutral translational energy distributions[16] before comparison with the data. The parameters n, σ_o, and E_0 are allowed to vary freely to best fit the data as determined by a nonlinear least-squares analysis. For analyses of some small cross sections, it was necessary to fix the value of n over an acceptable range while allowing σ_o and E_0 to vary freely. It is possible that this could introduce systematic errors in the thresholds determined, but the range of n values chosen in each case is large enough to include all likely possibilities. Errors in threshold values are determined by the variation in E_0 among several data sets for all acceptable models and the absolute uncertainty in the energy scale. These errors are believed to be reasonable measures of the absolute accuracy of the threshold values. The general form of eq 1 has been derived as a model for translationally driven reactions[28] and has been found to be quite useful in describing the shapes of endothermic reaction cross sections and in deriving accurate thermochemistry (within the stated error limits) for a wide range of systems.[29]

At elevated energies, some of the observed reaction cross sections decline with increasing energy. This can be due either to dissociation of the product ion or to competition with other product channels. These cross sections are reproduced by using a model for product dissociation which makes a simple statistical assumption within the constraints of angular momentum conservation.[30] The model is controlled by two parameters: p which is an adjustable parameter and E_D which is the energy at which the product begins to decompose or competition begins.

Derivation of Bond Energies. The 0 K threshold energy, E_0, for a reaction like process 2 is converted to bond energies at 0 K by using eq 3.

(17) Teloy, E.; Gerlich, D. *Chem. Phys.* **1974**, *4*, 417.
(18) Chantry, P. J. *J. Chem. Phys.* **1971**, *55*, 2746.
(19) Ervin, K. M.; Armentrout, P. B. *J. Chem. Phys.* **1987**, *86*, 2659.
(20) Schultz, R. H.; Armentrout, P. B. *Int. J. Mass Spectrom. Ion Processes* **1991**, *107*, 29.
(21) Sunderlin, L. S.; Armentrout, P. B. *J. Phys. Chem.* **1988**, *92*, 1209.
(22) Aristov, N.; Armentrout, P. B. *J. Phys. Chem.* **1987**, *91*, 6178.
(23) Chen, Y. M.; Clemmer, D. E.; Armentrout, P. B. *J. Chem. Phys.* **1993**, *98*, 4929.
(24) Clemmer, D. E.; Chen, Y. M.; Aristov, N.; Armentrout, P. B. *J. Phys. Chem.* **1994**, *98*, 7538.
(25) van Koppen, P. A. M.; Kemper, P. R.; Bowers, M. T. *J. Am. Chem. Soc.* **1992**, *114*, 10941.
(26) Georgiadis, R.; Armentrout, P. B. *J. Phys. Chem.* **1988**, *92*, 7067.
(27) Kemper, P. R.; Bowers, M. T. *J. Phys. Chem.* **1991**, *95*, 5134.
(28) Chesnavich, W. J.; Bowers, M. T. *J. Phys. Chem.* **1989**, *79*, 900.
(29) Armentrout, P. B. In *Advances in Gas Phase Ion Chemistry*; Adams, N. G., Babcock, L. M., Eds.; JAI, Greenwich, 1992; Vol. 1, p 83.
(30) Weber, M. E.; Elkind, J. L.; Armentrout, P. B. *J. Chem. Phys.* **1986**, *84*, 1521.

Table 2. Heats of Formation and Ionization Energies at 0 K[a]

species	$\Delta_f H_0$, eV	IE, eV
H	2.239	
SiH_4	0.46(0.02)	
SiH_3	2.14(0.03)[b]	8.135(0.005)[c]
SiH_2	2.85(0.07)[d]	
SiH	3.92(0.04)[e]	
Si	4.66(0.03)[f]	
CH_4	−0.688(0.004)	
$(CH_3)SiH_3$	−0.11(0.04)[g]	
TiH		6.48(0.14)[h]
VH		6.81(0.10)[i]
CrH		7.33(0.12)[i]

[a] All values except where noted are from ref 52. Uncertainties are in parentheses. [b] Seetula, J. A.; Feng, Y.; Gutman, D.; Seakins, P. W.; Pilling, M. J. *J. Phys. Chem.* **1991**, *95*, 1658. The 0 K value given above has been converted from a $\Delta_f H_{298}$ value using a calculated enthalpy change of $\Delta_f H(0) - \Delta_f H(298) = 0.059$ eV, which accounts for the translational, rotational, and vibrational heat capacities but not the electronic as the necessary molecular information is not available. Vibrational frequencies are taken from: Ho, P.; Coltrin, M. E.; Binkley, J. S.; Melius, C. F. *J. Phys. Chem.* **1985**, *89*, 4647. [c] Johnson, R. D.; Tsai, B. P.; Hudgens, J. W. *J. Chem. Phys.* **1989**, *91*, 3340. [d] Frey, H. M.; Walsh, R.; Watts, I. M. *J. Chem. Soc., Chem. Commun.* **1986**, 1189. The 0 K value given above has been converted from a $\Delta_f H_{298}$ value using a calculated enthalpy change $\Delta\Delta_f H(0-298) = 0.017$ eV, see footnote *b*. Vibrational frequencies are taken from: Fredlin, L.; Hauge, R. H.; Kafafi, Z. H.; Margrave, J. L. *J. Chem. Phys.* **1985**, *82*, 3542. [e] Berkowitz, J.; Russic, B. In *Vacuum Ultraviolet Photoionization and Photodissociation of Molecules and Clusters*; Ng, C. Y., Ed.; World Scientific: Singapore, 1991; pp 1−41. The 0 K value given above has been converted from a $\Delta_f H_{298}$ value using a calculated enthalpy change $\Delta\Delta_f H(0-298) = -0.018$ eV. Enthalpy content taken from ref 52. [f] Fisher, E. R.; Kickel, B. L.; Armentrout, P. B. *J. Phys. Chem.* **1993**, *97*, 10204. [g] Doncaster, A. M.; Walsh, R. *J. Phys. Chem.* **1979**, *83*, 3037. The $\Delta_f H_{298}$ value given in this reference is converted to a 0 K heat of formation by using the enthalpy change for ethane. [h] Chen, Y. M.; Clemmer, D. E.; Armentrout, P. B. *J. Chem. Phys.* **1991**, *95*, 1228. The 298 K IE (6.59 ± 0.14 eV) listed in this reference is converted to the 0 K value presented here. See ref 48. [i] Reference 23.

$$M^+ + BC \rightarrow MB^+ + C \quad (2)$$

$$D_0(M^+-B) = \Delta_f H_0(B) + \Delta_f H_0(C) - \Delta_f H_0(BC) - E_0 \quad (3)$$

This expression assumes that there are no activation barriers in excess of the endothermicity of the reaction. This assumption is generally reasonable for ion−molecule reactions and has been explicitly tested on a number of occasions.[29] The required literature thermochemistry for the silicon species is listed in Table 2.

Results

Ground State Reactions. Product cross sections for the reactions of SiH_4 with Ti^+, V^+, and Cr^+ produced in the DC/FT or SI ion sources are shown as a function of translational energy in Figures 1−3. In all systems, we observe reactions 4−9, where M refers to Ti, V, or Cr. In the Ti^+ system, reaction

$$M^+ + SiH_4 \rightarrow MH^+ + SiH_3 \quad (4)$$
$$\rightarrow MSi^+ + 2H_2 \quad (5)$$
$$\rightarrow MSiH^+ + H_2 + H \quad (6)$$
$$\rightarrow MSiH_2^+ + H_2 \quad (7)$$
$$\rightarrow MSiH_3^+ + H \quad (8)$$
$$\rightarrow SiH_3^+ + MH \quad (9)$$

9 is observed only at energies above 10 eV with a cross section that never exceeds 0.01 Å ^{2}. The adduct, $MSiH_4^+$, was not observed in any system, establishing that its cross section is below 0.01 Å^2.

There are two complexities associated with analyzing the cross sections for these systems. First, because silicon in natural abundance exists as ^{28}Si (92.27%), ^{29}Si (4.68%), and ^{30}Si (3.05%) isotopes, the results obtained for a given *m/z* ratio can represent several product species. This is straightforward to account for, and the cross sections presented here are total cross sections for all isotopes of a single chemical species.[31] Second, in order to accurately determine absolute magnitudes of product cross sections, ion transmission must be maximized, but this can require mass resolution conditions that do not completely separate signals from adjacent masses. In the present study, cross sections were measured under high resolution conditions

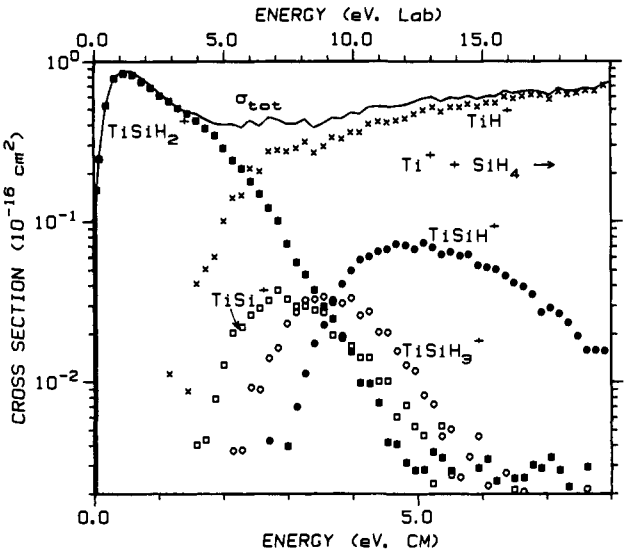

Figure 1. Variation of product ion cross sections for the reaction of Ti^+ (produced in the flow tube/dc-discharge source) with silane as a function of translational energy in the laboratory frame (upper scale) and center-of-mass frame (lower scale).

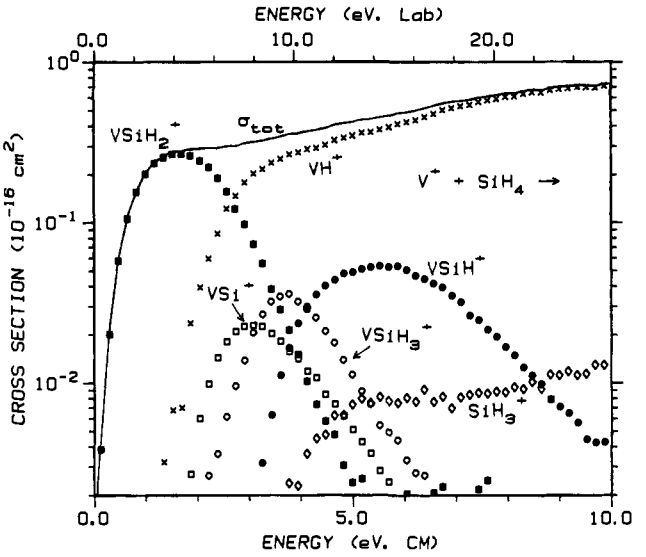

Figure 2. Variation of product ion cross sections for the reaction of V^+ (produced in the flow tube/dc-discharge source) with silane as a function of translational energy in the laboratory frame (upper scale) and center-of-mass frame (lower scale).

(31) For example, in the case of $^{48}Ti^+$, the product at *m/z* 77 can be due to $Ti^{28}SiH^+$ and $Ti^{29}Si^+$. The cross section for $Ti^{29}Si^+$ is calculated by taking the cross section for *m/z* 76 (due exclusively to $Ti^{28}Si^+$) and scaling it by the ^{28}Si:^{29}Si isotope ratio, 0.051. Subtraction of this cross section from the *m/z* 77 cross sections yields the cross section due entirely to $Ti^{28}SiH^+$. A similar procedure can then be followed for the *m/z* 78 (due to $Ti^{28}SiH_2^+$, $Ti^{29}SiH^+$, and $Ti^{30}Si^+$) and *m/z* 79 (due to $Ti^{28}SiH_3^+$, $Ti^{29}SiH_2^+$, and $Ti^{30}SiH^+$) cross sections. The cross sections for $Ti^{28}SiH_x^+$ product ions are then scaled by 1.084 (accounting for the natural abundance of ^{28}Si) to yield the results presented here for a single chemical species. This same general procedure was used for all three metal systems.

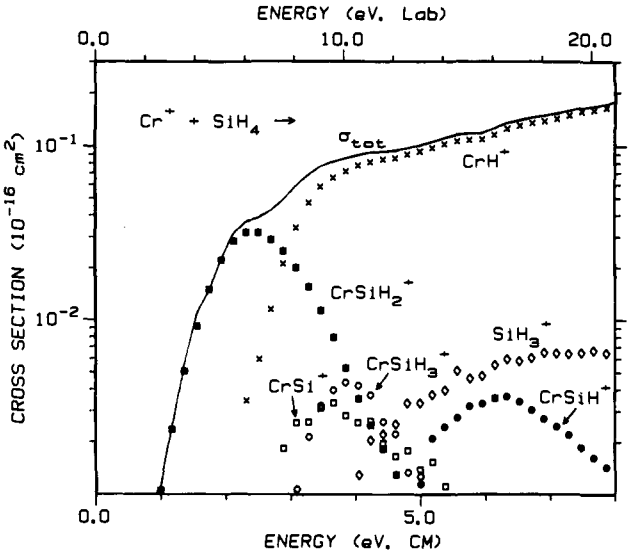

Figure 3. Variation of product ion cross sections for the reaction of Cr^+ (produced by surface ionization at 1900 K) with silane as a function of translational energy in the laboratory frame (upper scale) and center-of-mass frame (lower scale).

(<10% overlap between ions one mass unit apart) to determine the relative intensity of the products and under low mass resolution conditions (sufficiently low that further reductions in resolution do not enhance the product intensity) to verify efficient product collection. Because the kinetic energy dependence of different product ions is generally very distinct, it is straightforward and unambiguous to correct the cross sections for any deficiencies discovered by this comparison.

The overall reactivity in these systems is very similar (Figures 1–3). The dominant process at low energies is formation of $MSiH_2^+$, reaction 7. Comparison of this cross section in the Ti^+, V^+, and Cr^+ systems shows that production of $MSiH_2^+$ is least endothermic and therefore most efficient in the Ti^+ reaction. As the production of $MSiH_2^+$ becomes more endothermic, the magnitude of this cross section decreases, such that the $CrSiH_2^+$ cross section is ~30 times smaller at its maximum than the cross section for $TiSiH_2^+$. The cross section for $MSiH_2^+$ declines rapidly above ~2 eV in all three systems and the cross section for the formation of MH^+ increases concomitantly, demonstrating that these two processes compete. Furthermore, the shapes of the total cross sections indicate that the formation of $MSiH_2^+$ is closely coupled with that of MH^+, suggesting that they come from a common intermediate. The apparent thresholds for $MH^+ + SiH_3$ formation, reaction 4, are consistent with calculated values of 1.61 ± 0.12, 1.87 ± 0.07, and 2.55 ± 0.10 eV (Tables 2 and 3) for ground-state Ti^+, V^+, and Cr^+, respectively. This helps to confirm that the DC/FT source produces ground-state Ti^+ and V^+ reactant ions. The apparent thresholds (not visible on the logarithmic scale of Figures 2 and 3) for the competing $SiH_3^+ + MH$ formation, reaction 9, for M = V and Cr are consistent with the calculated values of 3.19 ± 0.08 and 3.36 ± 0.08 eV for ground-state V^+ and Cr^+, respectively. The failure to observe appreciable amounts of $SiH_3^+ + MH$ for M = Ti is discussed further below.

Reactions 5, 6, and 8 occur at higher energies and are relatively inefficient in all three systems. Reactions 4–6 and 8 occur with essentially the same efficiency for Ti^+ and V^+. In the case of Cr^+, reactions 6 and 8 are less efficient by nearly an order of magnitude. The smooth appearance of the sum of the cross sections for $MSiH^+$ and $MSiH_3^+$ products when M = Ti and V suggests that these two products are closely coupled. The total cross section for these products for Cr^+ is not a smooth function, implying that another process may be competing with the coupling between the $CrSiH^+$ and $CrSiH_3^+$ products, as discussed further below.

Table 3. Experimental Bond Energies at 0 K (eV)[a]

L	$D(Ti^+-L)$	$D(V^+-L)$	$D(Cr^+-L)$
H	2.31(0.11)[b]	2.05(0.06)[c]	1.37(0.09)[d]
C	4.05(0.24)	3.82(0.10)	
CH	4.95(0.12)	4.88(0.10)	3.04(0.3)
CH_2	3.94(0.09)	3.37(0.06)	2.24(0.04)
CH_3	2.21(0.06)	2.00(0.15)	1.14(0.04)
Si[e]	2.54(0.17)	2.37(0.15)	2.10(0.16)
SiH[e]	2.30(0.11)	2.09(0.12)	1.02(0.29)
SiH_2[e]	2.17(0.07), ≥2.27(0.08)[f]	2.02(0.09)	0.99(0.14)
SiH_3[e]	1.69(0.18)	1.54(0.16)	0.78(0.18)

[a] Unless otherwise noted values are taken from ref 48. Uncertainties are listed in parentheses. [b] Elkind, J. L.; Armentrout, P. B. *Int. J. Mass Spectrom. Ion Processes* **1988**, *83*, 259. [c] Elkind, J. L.; Armentrout, P. B. *J. Phys. Chem.* **1985**, *89*, 5626. [d] Elkind, J. L.; Armentrout, P. B. *J. Chem. Phys.* **1987**, *86*, 1868. [e] This study. [f] Reference 5.

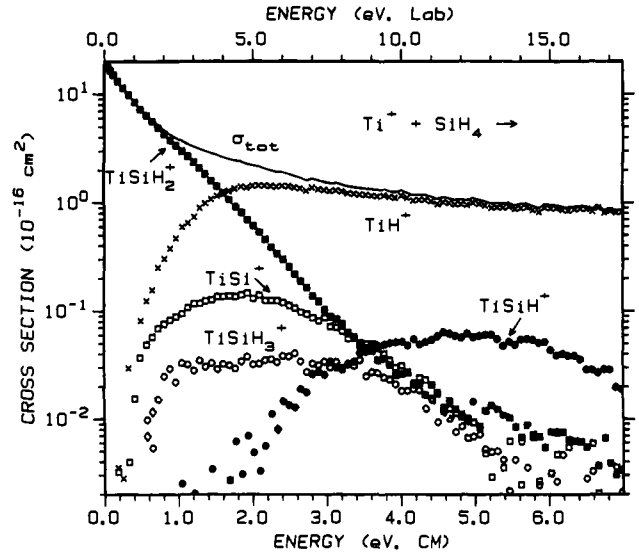

Figure 4. Variation of product ion cross sections for the reaction of Ti^+ (produced by 30 eV electron impact) with silane as a function of translational energy in the laboratory frame (upper scale) and center-of-mass frame (lower scale).

Excited State Reactions. Figures 4, 5, and 6 show data for Ti^+, V^+, and Cr^+, respectively, produced in the EI source. Comparison of Figures 4–6 to Figures 1–3 shows that excited electronic states enhance the reactivity of the Ti^+, V^+, and Cr^+ ions. Magnitudes for reactions 4, 5, and 7 increase by factors of 5, 4, and 21, respectively, for Ti^+; 7, 6, and 20, respectively, for V^+; and 6, 13, and 57, respectively, for Cr^+. Magnitudes for reactions 6 and 8 remain about the same for Ti^+ and V^+ while they increase by factors of 3 and 35, respectively, for Cr^+. The magnitude of reaction 9 increases slightly for V^+ and is unaffected by the reactivity of excited-state Cr^+ ions. For Ti^+, this reaction is now observed although the cross section is small (~0.01 Å^2) and nearly invariant with changes in the kinetic energy over the range shown in Figure 4.

The threshold energies for reactions 4–9 all shift to lower energies for the EI data. This is consistent with the electronic excitation of the reactant ion. The shift in threshold energies for the V^+ system, ~1.6 eV, is consistent with contributions from the a^3F and possibly higher-lying excited states, although contributions from the a^5F cannot be ruled out. In the Ti^+ system, the threshold shift of ~1.3 eV is indicative of contributions from the a^2F and possibly higher-lying excited states. The observed threshold shift for the Cr^+ system of ~2.5 eV indicates that there are contributions from the a^4D, a^4G, and possibly

Table 4. Summary of Optimum Parameters in Eq 1[a]

reaction	E_0, eV	n	σ_0	p	E_D
Ti^+(FT/DC)[b] + SiH_4 →					
$TiH^+ + SiH_3$	1.61(0.12)[c]	1.5(0.5)*	0.30(0.05)		
$TiSi^+ 2H_2$	1.66(0.17)	1.5(0.5)*	0.08(0.02)	2.3	2.8(0.2)
$TiSiH^+ + H_2 + H$	3.40(0.10)	0.9(0.3)	0.28(0.03)	1−3	5.2(0.2)
$TiSiH_2^+ + H_2$	0.22(0.02)	0.4(0.1)	0.53(0.06)	2	1.6(0.1)
$TiSiH_3^+ + H$	2.23(0.18)	1.5(0.5)*	0.09(0.03)	1−4	3.5(0.1)
V^+(FT/DC)[b] + SiH_4 →					
$VH^+ + SiH_3$	1.97(0.03)	1.1(0.1)*	0.50(0.03)		
$VSi^+ + 2H_2$	1.83(0.14)	1.5(0.5)*	0.06(0.02)	2,3	3.0(0.1)
$VSiH^+ + H_2 + H$	3.61(0.11)	1.0(0.3)*	0.18(0.02)	1,2	5.7(0.2)
$VSiH_2^+ + H_2$	0.37(0.06)	1.7(0.2)	0.34(0.05)	1,2	1.6(0.1)
$VSiH_3^+ + H$	2.38(0.16)	1.8(0.5)	0.10(0.03)	2−4	3.6(0.1)
$SiH_3^+ + VH$	3.19(0.07)[c]	1.3(0.3)*	0.02(0.01)		
Cr^+(SI) + SiH_4 →					
$CrH^+ + SiH_3$	2.58(0.12)	1.3(0.3)*	0.19(0.04)		
$CrSi^+ + 2H_2$	2.10(0.15)	1.5(0.5)*	0.01(0.005)	2,3	3.7(0.2)
$CrSiH^+ + H_2 + H$	4.68(0.29)	1.4(0.7)*	0.02(0.01)	1,2	6.1(0.3)
$CrSiH_2^+ + H_2$	1.40(0.12)	1.5(0.5)*	0.08(0.02)	2	2.4(0.1)
$CrSiH_3^+ + H$	3.14(0.18)	1.5(0.5)*	0.05(0.04)	3,4	3.8(0.1)
$SiH_3^+ + CrH$	3.38(0.07)	1.3(0.3)*	0.01(0.005)		
Ti^+(EI)[d] + SiH_4 →					
$TiH^+ + SiH_3$	0.43(0.09)	1.8(0.3)*	1.3(0.3)		
$TiSi^+ + 2H_2$	0.28(0.06)	1.5(0.3)*	0.14(0.02)	2	1.9(0.1)
V^+(EI)[d] + SiH_4 →					
$VH^+ + SiH_3$	0.35(0.08)	1.7(0.2)	1.5(0.2)		
$VSi^+ + 2H_2$	0.37(0.10)	1.7(0.4)*	0.28(0.02)	1	1.4(0.1)
$VSiH^+ + H_2 + H$	1.94(0.20)	1.5(0.5)*	0.05(0.02)	1,2	5.0(0.4)
Cr^+(EI)[d] + SiH_4 →					
$CrH^+ + SiH_3$	0.15(0.03)	1.1(0.3)*	0.51(0.14)		
$CrSiH^+ + H_2 + H$	2.07(0.25)	2.1(0.3)*	0.02(0.01)	1,2	4.8(0.2)

[a] Uncertainties are in parentheses. Asterisks represent those analyses where the value of n is fixed over the indicated range, see text. [b] Ions generated in the flow tube/DC ionization source. [c] The value of E_0 was held constant to reproduce the cross section. [d] Ions generated in the electron impact (electron energy of 30 eV) ionization source. Threshold energies have not been corrected for electronic energy of the ionic reactant. Due to the number of reactant states present in the beam it was often difficult to model the cross section behavior. Therefore, only those cross sections which could be modeled accurately are listed here.

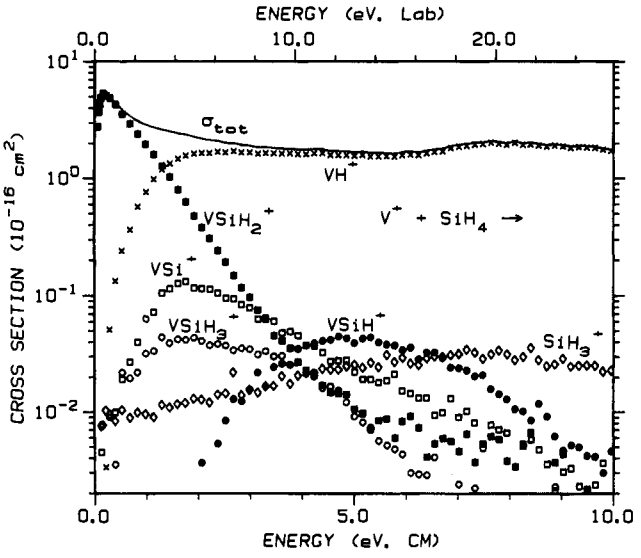

Figure 5. Variation of product ion cross sections for the reaction of V^+ (produced by 30 eV electron impact) with silane as a function of translational energy in the laboratory frame (upper scale) and center-of-mass frame (lower scale).

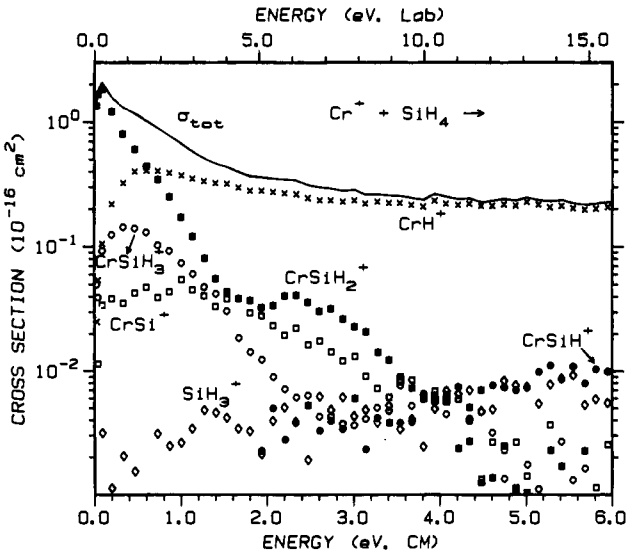

Figure 6. Variation of product ion cross sections for the reaction of Cr^+ (produced by 30 eV electron impact) with silane as a function of translational energy in the laboratory frame (upper scale) and center-of-mass frame (lower scale).

higher-lying excited states. Similar shifts in threshold energies have been observed for the reactions of methane with these metal ions produced in the same set of sources.[21,22,26]

Thermochemistry

The threshold regions of the cross sections for ground state data were analyzed by using eq 1. These analyses are summarized in Table 4, and in all cases, the model of eq 1 accurately reproduces the experimental results. Measured threshold energies, E_0, are combined with literature thermochemistry, listed in Table 2, in eq 3 to determine 0 K bond energies for M^+-SiH_x (x = 0−3). These bond energies are listed in Table 3. Because the EI data are a complex combination of the reactivities of several electronic states, analyses of the cross sections with eq 1 do not lead to useful thermochemistry but can be used to assess the average electronic excitation

by measuring the shift in threshold energies compared to the flow tube data. Results of such analyses are also listed in Table 4.

Few M^+-SiH_x bond energies have been determined previously. The only M^+-SiH_x bond energy related to the present study was determined by Kang *et al.*[5] They investigated the reaction of Ti^+ with methylsilane and concluded that formation of $TiSiH_2^+ + CH_4$ was exothermic, placing a lower limit of 2.27 ± 0.08 eV[32] on the Ti^+-SiH_2 bond energy. This value is slightly greater than the $TiSiH_2^+$ bond energy derived in the present study. The limit of Kang *et al.* is not a rigorous one because the exothermic reactivity that they observed could be due to excited states. Kang *et al.* generated Ti^+ by surface ionization at 2290 K leading to 62% a^4F ground state (average electronic energy of 0.026 eV), 36% b^4F (0.134 eV), 2% a^2F (0.591 eV), and higher-lying excited states. Kang *et al.* also investigated the reactions of V^+ and Cr^+ with silane and observed no reactions at 0.5 eV for either system, consistent with the present results. We do not observe any reactivity of Cr^+ with silane at 0.5 eV and only a small, ≤ 0.05 Å^2, reactivity for V^+, below the detection limit of the previous experiment. Having derived bond energies for the various $MSiH_x^+$ species (Table 3), the energy dependences of the individual product cross sections can now be analyzed in more detail. This is done in the following sections.

MH^+ and SiH_3^+. As mentioned above, the thresholds for $MH^+ + SiH_3$ formation, reaction 4, and for $MH + SiH_3^+$, reaction 9, are consistent with known thermochemistry. The failure to observe appreciable amounts of SiH_3^+, reaction 9, for ground-state M = Ti reactants has two plausible explanations. One possibility has to do with the difference in ionization energies (IEs) of MH and SiH_3 (Table 2). Because IE(TiH) is 1.6 eV lower than IE(SiH_3), the formation of $TiH^+ + SiH_3$ is strongly favored over $SiH_3^+ + TiH$. However, the IEs of VH and CrH are also lower than IE(SiH_3) by 1.3 and 0.8 eV, respectively, making formation of $MH^+ + SiH_3$ thermodynamically favored in all three systems. The second possibility has to do with the electronic configuration of the metal center. The formation of $SiH_3^+ + MH$ is a simple hydride (H^-) transfer reaction from SiH_4 to M^+ (although the mechanism may be more complex). Such a reaction may occur most readily when the metal ion has an empty 4s orbital,[33] because this avoids repulsive interactions between the 4s electron and the pair of H^- electrons. The a^4F ($4s3d^2$) ground state of Ti^+, unlike ground-state V^+ (a^5D, $3d^4$) and Cr^+ (^6S, $3d^5$), has an occupied 4s orbital. Therefore, the occupancy of the 4s orbital of Ti^+-(a^4F) may be a contributing factor to the inefficient formation of $SiH_3^+ + TiH$.

$MSiH_3^+$. The decline of the $MSiH_3^+$ cross sections at elevated kinetic energies is either a result of dehydrogenation to form $MSiH^+ + H_2$, reaction 6, or dissociation to $M^+ + SiH_3$, reaction 10.

$$M^+ + SiH_4 \rightarrow M^+ + SiH_3 + H \qquad (10)$$

Reaction 10 can begin at 3.92 ± 0.04 eV, while the thresholds measured for reaction 6 are 3.40 ± 0.10, 3.61 ± 0.11, and 4.68 ± 0.29 eV for Ti^+, V^+, and Cr^+, respectively (Table 4). Our analyses of the $TiSiH_3^+$ and $VSiH_3^+$ cross sections yield E_D values consistent with the onset of reaction 6. This, combined with the smooth appearance of the sum of the $MSiH_3^+$ and $MSiH^+$ cross sections, verifies that the $MSiH_3^+$ products dehydrogenate at higher energies for M = Ti and V. In the case of Cr^+, the decline in the $MSiH_3^+$ occurs well before the onset of reaction 6. The analysis of the $CrSiH_3^+$ cross section yields $E_D = 3.8 \pm 0.3$ eV, consistent with the onset of reaction 10. Because of the competition with reaction 10, the close coupling between the $MSiH_3^+$ and $MSiH^+$ product channels observed for M = Ti and V is not evident for M = Cr.

$MSiH_2^+$. The endothermicity for formation of $TiSiH_2^+ + H_2$ is sufficiently small that this cross section reaches a maximum at very low energies and then declines as $E^{-1/2}$, behavior expected for a near-thermoneutral reaction.[34] The $VSiH_2^+$ and $CrSiH_2^+$ cross sections do not exhibit this behavior because the endothermicities are higher. These two product cross sections reach maxima at energies determined by competition with formation of $MH^+ + SiH_3$ in reaction MH. This competition also explains why the $TiSiH_2^+$ cross section begins to decline more rapidly above ~2 eV. Analysis of the $TiSiH_2^+$ cross section shows a decline beginning at $E_D = 1.6 \pm 0.1$ eV, which is consistent with the calculated threshold for TiH^+ formation of 1.61 ± 0.12 eV. The $VSiH_2^+$ cross section was best reproduced with a E_D of 1.6 ± 0.1 eV, slightly lower than the calculated threshold for VH^+ of 1.87 ± 0.06 eV. The $CrSiH_2^+$ analysis yielded $E_D = 2.4 \pm 0.1$ eV, which is consistent with the calculated threshold for CrH^+ formation of 2.55 ± 0.10 eV.

$MSiH^+$. The decline in the $MSiH^+$ cross sections could be due to reactions 10, 11, or 12. The thresholds for reactions 10 and 11 are 3.92 ± 0.04 and 5.70 ± 0.08 eV, respectively. The

$$M^+ + SiH_4 \rightarrow M^+ + SiH + H + H_2 \qquad (11)$$
$$\rightarrow MSi^+ + H_2 + H + H \qquad (12)$$

thresholds for reaction 12 are 6.14 ± 0.17, 6.31 ± 0.15, and 6.58 ± 0.16 eV for Ti^+, V^+, and Cr^+, respectively. Based on the dissociation energies, E_D, used to model these cross sections, reaction 11 appears to be largely responsible for the decline. Reaction 10 occurs at too low an energy to account for the decline, and reactions 12 have thresholds that are too high.

MSi^+. The MSi^+ cross sections begin to decline at kinetic energies of 3–3.5 eV. This is below the threshold for the decomposition reaction 13 at 4.16 ± 0.08 eV.

$$M^+ + SiH_4 \rightarrow M^+ + Si + 2H_2 \qquad (13)$$

Because MSi^+ must be formed by dehydrogenation of the $MSiH_2^+$ product, the decline in these cross sections is due to the depletion of its $MSiH_2^+$ precursor, which is largely due to competition with $MH^+ + SiH_3$ formation.

Comparison of M^+-CH_x and M^+-SiH_x bond energies. Table 3 lists the M^+-SiH_x bond energies measured here along with M^+-CH_x bond energies measured previously. Both metal–carbon and metal–silicon bond energies decrease with increasing number of hydrogen atoms and as the metal is changed from Ti^+ to V^+ to Cr^+. The metal–silicon bond energies are considerably weaker than the metal–carbon bond energies. This result is not surprising when one considers that bonds to silicon are generally weaker than those to carbon, and is also consistent with the theoretical calculations on $MSiH_2^+$.[8]

Previously we have discussed the trends exhibited by metal–carbon bond energies by comparing them to related organic species.[12,35] The relative bond energies of $D(H-CH_3)$, $D(CH_3-$

(32) Reference 5 cites a lower limit for this bond energy of 2.52 eV at a temperature of 298 K. To compare to the present results, the bond energy has been changed to a 0 K value by using the heats of formation listed in Table 2.

(33) Schultz, R. H.; Elkind, J. L.; Armentrout, P. B. *J. Am. Chem. Soc.* **1988**, *110*, 411.

(34) Ervin, K. M.; Armentrout, P. B. *J. Chem. Phys.* **1987**, *86*, 2659.

(35) Aristov, N.; Armentrout, P. B. *J. Am. Chem. Soc.* **1984**, *106*, 4065.

CH_3), $D(CH_2{=}CH_2)$, $D(CH{\equiv}CH)$, and $D(C{-}C)$ are 1.0:0.9:1.7:2.2:1.4. The bond energies of $D(M^+{-}H)$, $D(M^+{-}CH_3)$, $D(M^+{-}CH_2)$, $D(M^+{-}CH)$, and $D(M^+{-}C)$ are related as 1.0:0.9:1.7:2.3:1.8 (average values for M = Ti, V, and Cr, which all have similar ratios). The bond energy relationships of the organic species are consistent with the multiple bonding exhibited by these species. Therefore we take the similarities of the organic and metal−carbon bond energy relationships to indicate that MH^+ and MCH_3^+ are singly bonded, MCH_2^+ and MC^+ are doubly bonded, and MCH^+ is triply bonded.[21] The bond energies of $D(M^+{-}H)$, $D(M^+{-}SiH_3)$, $D(M^+{-}SiH_2)$, $D(M^+{-}SiH)$, and $D(M^+{-}Si)$ are related as 1.0:0.7:0.9:0.9:1.3 (average for M = Ti, V, and Cr, which all have similar ratios except for MSi^+ where the specific ratios are 1.1 for $TiSi^+$ and VSi^+ vs 1.5 for $CrSi^+$ relative to MH^+). Clearly, the metal−silicon bond energy relationships are different from the organic and metal−carbon bond energy relationships. Direct comparison of the metal−silicon and metal−carbon relationships (both relative to MH^+) shows that the metal−silicon single bond is weaker than the metal−carbon analogue and that the formation of multiple bonds is less facile for Si than C.

Because the metal−carbon and metal−silicon bond energy relationships are so different, comparison of the metal−silicon species to the organic analogues provides no insight into the bonding mechanisms of the metal−silicon species. A more useful comparison is to the silicon−silicon bonded analogues. The bond energies of $D(H{-}SiH_3)$, $D(SiH_3{-}SiH_3)$,[36] $D(H_2Si{-}SiH_2)$,[37] $D(HSi{-}SiH)$,[38] and $D(Si{-}Si)$[39] are related as 1.0:0.8:0.8:1.0:0.8. These silicon−silicon bond energy relationships illustrate the difficulty silicon has in forming multiple bonds because they do not increase as for the single, double, and triple bonds of the analogues carbon species. Comparison of these silicon−silicon bond energy relationships to those of the metal-silicon relationships shows a reasonably parallel sequence, which may indicate that the bonding interactions between metal ions and silicon ligands are largely covalent. We note that metal−silylene ion BDEs are slightly stronger than those for metal−silyl ions and $H_2Si{-}SiH_2$. This might be explained by contributions from dative bonding, which corresponds to electron configurations where the $SiH_2(^1A_1)$ ground state bonds to the metal ions by donating its a_1 lone pair of electrons into empty metal 4s or 3dσ orbitals accompanied by 3dπ back-donation from the metal to the empty b_1 orbital on SiH_2. Such ideas are explored in more detail in the theoretical calculations of Cundari and Gordon,[8] who conclude that the $M^+{-}SiH_2$ bond for Ti^+, V^+, and Cr^+ is largely (45%) described as a covalent double bond with appreciable (35%) ylide−like ($M^{2+}{-}SiH_2^-$, corresponding to a high-energy asymptote) contributions where there is both a dative σ bond and a *covalent* (rather than a dative) double bond. Dative bonding may also contribute to the interactions between the metal ions and $SiH(^2\Pi)$ or $Si(^3P)$. The relative strength of the $M^+{-}Si$ bonds (especially $CrSi^+$) may indicate a different bonding mechanism than the other $M^+{-}SiH_x$ species.

A further complication in understanding the trends in these bond energies is the possibility that some of the hydrogens are bonded directly to the metal, e.g. $H{-}M^+{-}SiH_2$ instead of $M^+{-}SiH_3$, or that they bridge the metal and silicon atom. The first possibility cannot be ruled out entirely, although it seems unlikely because the metal−hydrogen bond energies (Table 3) are all weaker than even the weakest silicon−hydrogen bond, $D(H_2Si{-}H) = 2.95$ eV (Table 2). Bridging hydrogens are known to be important in $Si_2H_4^+$, Si_2H_4, and Si_2H_2 species.[40-42] In the Si_2H_4 case, the ethene-like structure is calculated to be the ground-state structure but the double-bridged isomer, $HSi(H)_2SiH$, is a local minimum about 1 eV higher in energy. In the Si_2H_2 case, calculations indicate that the monobridged Si(H)SiH, disilavinylidene (H_2SiSi), and *trans*-HSiSiH isomers all lie within 0.9 eV of the ground-state double-bridged $Si(H_2)$-Si structure. The present results cannot be used to ascertain which of the MH_xSi^+ structures or bonding mechanisms may be most important.

Discussion

Comparison with the Reactions of Ti^+, V^+, and Cr^+ with Methane. To better understand the effects that substitution of Si for C can have in organotransition-metal bonding, we can compare our present results with those for the reactions of Ti^+, V^+, and Cr^+ with methane.[21,22,26] Not surprisingly, the general reactivities observed in the present results are similar to those previously observed for reactions with methane.[21,22,26] The lowest energy product observed is $MCH_2^+ + H_2$ whereas MH^+ dominates the reactivity at higher energies. Minor products include MCH_x^+ ($x = 1$ and 3 for Ti^+ and V^+ and $x = 3$ for Cr^+), however, no MC^+ nor $CrCH^+$ products are observed. The overall total reactivity of the silane systems is greater with total cross sections approximately 3, 2, and 4 times greater for M = Ti, V, and Cr, respectively, than in the reactions with methane. This increase in total reactivity is reasonable as the Si−H bonds of silane are weaker than the C−H bonds in methane.

Interestingly, MXH_2^+ (X = Si or C) cross sections in the methane systems contribute considerably less to the total reactivity than in the silane systems. There are three factors that might explain this observation. First, production of MXH_2^+ is thermodynamically more favorable in the silane systems because dehydrogenation of silane requires 2.39 eV while dehydrogenation of methane requires 4.71 eV. Second, silylene has a $^1A_1$ ground state and a low-lying $^3B_1$ state,[43] whereas the ground state of methylene is $^3B_1$. As discussed above, the $^1A_1$ state can readily form a dative σ bond by donating nonbonding electrons into an empty 4s or 3dσ on the metal atom. The $^3B_1$ states bind preferentially by forming covalent σ and π bonds to the metal. Third, previous work in our laboratory and others has demonstrated that hydrogen atom migrations are facile on silicon centers.[40,44,45] The increased hydrogen mobility at silicon centers could enhance the dehydrogenation process in the silane systems as compared to the methane systems.

Reaction Mechanism. The results can be understood by assuming that M^+ reacts with silane by inserting into a Si−H bond to form intermediate **I**, $H{-}M^+{-}SiH_3$. The analogous intermediate has been suggested previously for reactions of Ti^+, V^+, and Cr^+ with CH_4.[21,22,26] Although the structure of **I** is a reasonable choice for the reaction intermediate, it is possible that bridged isomers, e.g. $M^+(H)SiH_3$ or $M^+(H_2)SiH_2$, are involved instead, as discussed above. The present results cannot be used to ascertain which of the MH_4Si^+ structures may be

(36) $\Delta_fH_0(Si_2H_6) = 1$ eV taken from Lias, S. G.; Bartmess, J. E.; Liebman, J. F.; Holmes, J. L.; Levin, R. D.; Mallar, W. G. *J. Phys. Chem. Ref. Data* **1988**, *17*, No. 1.

(37) Kutzelnigg, W. *Angew. Chem., Int. Ed. Engl.* **1984**, *89*, 272.

(38) Ruscic, B.; Berkowitz, J. *J. Chem. Phys.* **1991**, *95*, 2416.

(39) Huber, K. P.; Herzberg, G. *Molecular Spectra and Molecular Structure Constants of Diatomic Molecules*; Van Nostrand Reinhold Company: New York, 1979, and references therein.

(40) Boo, B. H.; Armentrout, P. B. *J. Am. Chem. Soc.* **1987**, *109*, 3549.

(41) Trinquier, G. *J. Am. Chem. Soc.* **1990**, *112*, 2130 and references therein.

(42) Grev, R. S.; Schaefer, H. F. *J. Chem. Phys.* **1992**, *97*, 7990.

(43) Berkowitz, J.; Greene, J. P.; Cho, H. *J. Chem. Phys.* **1987**, *86*, 1235.

(44) Kickel, B. L.; Fisher, E. R.; Armentrout, P. B. *J. Phys. Chem.* **1992**, *96*, 2603.

(45) Mandich, M. L.; Reents, W. D., Jr.; Jarrold, M. F. *J. Chem. Phys.* **1988**, *88*, 1703. Mandich, M. L.; Reents, W. D., Jr.; Kolenbrander, K. D. *J. Chem. Phys.* **1990**, *92*, 437.

the most important, but the competition between the various product channels and the state-specific chemistry is easily understood in terms of an intermediate like **I**. Therefore, the remainder of this discussion proceeds by assuming that the primary reaction intermediate has structure **I** without necessarily implying that other structures are not involved.

There are two possible mechanisms for the dehydrogenation of **I** to form $MSiH_2^+$. One possibility involves hydrogen migration to form intermediate **II**, $H_2M^+-SiH_2$, followed by reductive elimination of molecular hydrogen. A similar intermediate was discounted in the methane reactions based on thermodynamic considerations and the fact that Ti^+ doesn't have enough valence electrons (3) to form a covalently bound structure like **II** if the Ti−C bond is a double bond. However, because of the decreased strength of the Si-H bonds, the greater mobility of hydrogen atoms on silicon centers,[40,44,45] and the possibility that $SiH_2(^1A_1)$ can form a simple donor bond with M^+, intermediate **II** is a more reasonable possibility in the silane systems than in methane systems. The second possibility is a four-centered elimination of molecular hydrogen from **I**, which should be considered for several reasons. First, for the reactions of Ti^+, V^+, and Cr^+ with methane,[21,22,26] we concluded that formation of MCH_2^+ occurred via a four-centered elimination. Second, if **II** were being formed, we might have observed formation of MH_2^+, which was not the case, although this product is observed for the group 3 metal ions[46] where it is thermodynamically more favorable.[47,48] Third, theoretical calculations have demonstrated that a four-centered elimination can occur with little or no barrier if the metal−ligand bonds are covalent and have substantial d character, as would be the case in **I**.[49] We conclude that formation of $MSiH_2^+$ could proceed by either of these mechanisms, or similar species that have bridging hydrogens. Loss of molecular hydrogen from $MSiH_2^+$ results in formation of MSi^+.

The observed competition between formation of MH^+ and $MSiH_2^+$ in reactions 4 and 7, respectively, may be explained in terms of a common intermediate like **I**. At low energies, formation of $MSiH_2^+$ dominates, indicating that elimination of H_2 is thermodynamically favored. As the energy increases, decomposition of **I** through reaction 4 is kinetically favored despite being more endothermic because it goes through a loose transition state whereas reaction 7 proceeds through one of the more restricted mechanisms discussed above. The dominance of reaction 4 may also be understood in terms of conservation of angular momentum[22] and possible contributions from more direct pathways at the highest kinetic energies. Other higher energy decomposition pathways available to intermediate **I** include dissociation by simple bond cleavage to form MH + SiH_3^+ or $MSiH_3^+$ + H. Further decomposition of this latter product by dehydrogenation yields $MSiH^+$, as discussed above.

Molecular Orbital and Spin Considerations. As was the case in the reactions with methane,[21,22,26] the interaction of individual electronic states with silane may be understood by using simple molecular orbital arguments. Oxidative addition of a Si−H bond to a metal center is achieved by donation of the bonding σ electrons into empty 4s and 3dσ orbitals of the metal and back-donation of metal 3dπ electrons into the σ^* antibonding orbital. This results in an increase of electron density between the metal and the molecular fragment and a lengthening of the Si−H bond. Furthermore, this simple picture would predict that metal states having an occupied 4s or 3dσ orbital will have repulsive interactions with the Si−H bonding σ electrons.

Spin conservation is another important factor to be considered in the reactivity of metal ions and can be used to rationalize the effect of electronic state for various product channels. Reactions 14−19 show the spin states of the individual species for the observed reactions where the number in parentheses is the spin quantum number of that particular species. The value of s is chosen to represent the ground state of the MH^+ product, therefore, s = 1, $^3/_2$, and 2 for TiH^+, VH^+, and CrH^+, respectively, indicating that these species have triplet, quartet, and quintet spins, respectively.[50,51] The indicated spin states for SiH_4, H_2, H, SiH_3^+, and MH are known.[39,52,53] Those for $MSiH_2^+$ have been calculated.[8] We assume that $MSiH_3$+ has a single M−Si covalent bond and therefore has the same spin state as MH^+. The spins for $MSiH^+$ and MSi^+ are assumed to be the same as their precursors, $MSiH_3^+$ and $MSiH_2^+$, respectively.

$$M^+(s \pm {}^1/_2) + SiH_4(0) \rightarrow MH^+(s) + SiH_3({}^1/_2) \quad (14)$$
$$\rightarrow MSi^+(s - {}^1/_2) + 2H_2(0) \quad (15)$$
$$\rightarrow MSiH^+(s) + H_2(0) + H({}^1/_2) \quad (16)$$
$$\rightarrow MSiH_2^+(s - {}^1/_2) + H_2(0) \quad (17)$$
$$\rightarrow MSiH_3^+(s) + H({}^1/_2) \quad (18)$$
$$\rightarrow SiH_3^+(0) + MH(s + {}^1/_2) \quad (19)$$

Therefore, reactions 15 and 17 are spin-allowed for low-spin ($s - {}^1/_2$) but not high-spin ($s + {}^1/_2$) states of M^+. This probably explains why reaction 17 exhibits the largest enhancement in the reactions of all three excited-state metal ions. The experimental observation that the high-spin ground states of Ti^+, V^+, and Cr^+ react with SiH_4 to form $MSiH_2^+ + H_2$ products implies that there must be spin−orbit coupling between the high- and low-spin surfaces. The relative inefficiency of the ground-state reactions compared with the low−spin excited states implies that this coupling is rather poor. Because the enhancement in reactivity observed for M = Cr is approximately 3 times greater than that observed for Ti or V, the coupling is the worst in the case of Cr. This can be rationalized by noting that the excitation energy to the reactive low-spin states changes from 0.6 eV for Ti^+ to 1.1 eV for V^+ to 2.4 eV for Cr^+, Table 1.

In contrast, reaction 19 is spin-allowed for high-spin M^+ ($s + {}^1/_2$) states only. Thus, low-spin M^+ can produce SiH_3^+ only through a surface crossing onto the high-spin surface, consistent with the lack of or very small enhancement observed in the production of SiH_3^+ by excited states. We also note that the electron configurations of the lowest energy low-spin states, $Ti^+(a^2F, 4s3d^2)$, $V^+(a^3F, 4s3d^3)$, and $Cr^+(a^4D, 4s3d^4)$, may not be suitable for efficiently accepting an H^- from SiH_4, as discussed above for Ti^+.

All three metal ions also show an enhanced excited-state reactivity for process 14, formation of MH^+, even though this reaction is spin-allowed from both ($s \pm {}^1/_2$) spin states of M^+. As noted above, this product shows competition with $MSiH_2^+$ formation indicating that a common intermediate to both processes is involved. If this intermediate has a low-spin ground

(46) Kickel, B. L.; Armentrout, P. B. *J. Am. Chem. Soc.* Submitted for publication.
(47) Sunderlin, L. S.; Armentrout, P. B. *J. Am. Chem. Soc.* **1989**, *111*, 3845.
(48) Armentrout, P. B.; Kickel, B. L. *Organometallic Ion Chemistry*; Freiser, B. S., Ed., in press.
(49) Steigerwald, M. L.; Goddard, W. A. *J. Am. Chem. Soc.* **1984**, *106*, 308.
(50) Schilling, J. B.; Goddard, W. A.; Beauchamp, J. L. *J. Am. Chem. Soc.* **1986**, *108*, 582.
(51) Petterson, L. G. M.; Bauschlicher, C. W.; Langhoff, S. R.; Partridge, H. *J. Chem. Phys.* **1987**, *87*, 481.
(52) Chase, M. W.; Davies, C. A.; Downey, J. R., Jr.; Frurip, D. J.; McDonald, R. A.; Syverud, A. N. *J. Phys. Chem. Ref. Data* **1985**, *14*, Supp. No. 1 (JANAF Tables).
(53) Pople, J. A.; Curtiss, L. A. *J. Phys. Chem.* **1987**, *91*, 155.

state, e.g., as would be likely for intermediate **I** if both bonds to the metal are covalent, then the excited-state enhancement is easily explained. Formation of **I** occurs diabatically from states having the correct spin and electronic configuration. The lowest states that meet these requirements are Ti^+ (a^2G, $3d^3$), V^+ (a^3P, $3d^4$), and Cr^+ (a^4G, $3d^5$). The enhancement in this reaction is presumably not as great as that observed for the $MSiH_2^+$ product because MH^+ can also be formed by spin-allowed pathways along high-spin ($s + 1/2$) surfaces.

The remaining reactions, processes 16 and 18, are also spin-allowed from both ($s \pm 1/2$) spin states of M^+. This can explain the observation that reactions 16 and 18 are not sensitive to excited electronic states for M = Ti and V, although this observation suggests that these processes do not rely on intermediate **I** as heavily as process 14. In contrast, reactions 16 and 18 are enhanced by excited electronic states for M = Cr, again consistent with reactions occurring via intermediate **I**. The disparate behavior among the three metal systems is probably related to the difference in coupling between high- and low-spin surfaces attributable to the large difference in excitation energies noted above.

Summary

In this study, we examine the reactions of Ti^+, V^+, and Cr^+ with silane. Threshold analyses of the cross sections allow the derivation of 0 K bond dissociation energies for M^+-SiH_x ($x = 0-3$). In all cases, the metal−silicon bond energies are significantly weaker than analogous metal−carbon bond energies. Comparison of trends in carbon−carbon, metal−carbon, silicon−silicon, and metal-silicon bond energies suggest that the bonding of $MSiH_x^+$ ($x = 0-2$) species may be largely described as covalent interactions, although these conclusions are clouded by uncertainties in the structures of the $MSiH_x^+$ species and by likely contributions from dative bonding interactions.

We find that the reactions are more efficient for low-spin doublet (Ti^+), triplet (V^+), and quartet (Cr^+) excited states, results that suggest the existence of a low-spin intermediate. Although the results may be understood in terms of an intermediate having a $H-M^+-SiH_3$ structure, it is possible that bridged isomers, $M^+(H)SiH_3$ or $M^+(H_2)SiH_2$, are involved as well. Although formation of this intermediate is spin-forbidden from the high-spin quartet (Ti^+), quintet (V^+), and sextet (Cr^+) ground states, these states are observed to react to form low-spin products, indicating that spin-orbit coupling to the low-spin surfaces does occur.

Acknowledgment. This work was supported by the National Science Foundation under Grant No. CHE-9221241.